

Modeling and Simulation of Olefin Polymerization at Microstructure Level

*Dashti, Ali; Ramazani S.A., Ahmad***

*Polymer Engineering Group, Department of Chemical and Petroleum Engineering,
Sharif University of Technology, P.O. Box 11155-9465 Tehran, I.R. IRAN*

ABSTRACT: *A new model based on a combination of the polymeric multigrain and multilayer models has been developed to predict the polymerization rate, particle growth, morphology, effective parameters on broadening of the molecular weight distribution, number and weight average of the molecular weight, isotacticity index and bulk density of polymer. Mathematical correlations and the kinetics used in this model are based on the polymeric multigrain and the multilayer models, respectively. In the modeling, multiplicity of active site using different kinetics parameters as well as deactivation of catalyst during the polymerization have been considered,. Moreover, it considers mass transfer effects on polymerization characteristics. The Effects of physico-chemical aspects of catalyst associated with the polymerization in slurry phase are also considered in this model. In addition, the effects of more important model parameters including time step, number of layers and number of active sites on the produced polymer features are reviewed. The model predictions show that propagation rate constant, multiplicity of active site, concentration of any individual active site type, and the initial size of the catalyst particles have considerable effects on the properties of the final polymer. The results obtained from simulation with this new combined model confirm at least better qualitative prediction of the polymerization characteristics in comparison with simulation results of the multigrain model (MGM) and the two models mentioned above.*

KEY WORDS: *Modeling, Simulation, Polyolefin, Polymerization, Microstructure, Ziegler-Natta .*

INTRODUCTION

Polyolefins, especially polypropylene and polyethylene are the most important polymers, as they comprise about 60 % of the total thermoplastics world's markets strongly demand and are mostly produced by use of heterogeneous Ziegler-Natta catalyst systems.

Heterogeneous Ziegler-Natta catalysis has proven to be a remarkably versatile technology for polymerization of α -olefins; nowadays, irrespective of the advent of

homogeneous metallocene catalysts for the polyolefin production, use of Ziegler-Natta catalysts is still increasing. Hence, understanding of the olefin polymerization by this catalyst system seems to be a crucial objective for the control, optimization and improvement of process performance for the modern and conventional plants in both aspects of kinetic and transport phenomena.

In Ziegler - Natta olefin polymerization, olefin

* To whom correspondence should be addressed.

+ E-mail: ramazani@sharif.edu

1021-9986/08/2/13

10/\$/3.00

monomers reach active sites on the surface of the catalyst particles, in which polymerization occur, by adsorption and diffusion. According to the catalyst fragmentation theory, the stress generating from the growing polymer molecules breaks down the catalyst structure when enough polymers are produced.

Based on this phenomenon, there are several important factors that affect the polymer morphology. The most important aspects affecting the polymerization kinetics and transport phenomena are: type of active site, active site concentration, cocatalyst concentration, and polymerization conditions such as pressure, temperature and prepolymerization conditions [1,2].

Among the various models with a single type of active site on the catalyst surface, the simplest forms are the core models like solid and polymeric core models, which show high deviation from real behavior of polymerization systems. In the solid core model, polymerization occurs at the surface of an inner core and the resulting polymer is assumed to accumulate around a catalyst sphere with the monomer diffusing through the growing dense polymeric layer; while in the polymeric core model, the polymerization occurs through the active site of the catalyst. The active sites are distributed uniformly through a stationary inner polymer sphere and could move slowly in an indefinite direction [4]. For the later model, the predicted results have shown unity of the polydispersity in spite of the experimental observations. The obvious reason arises from the absence of termination kinetics in the mentioned model.

To develop more realistic models, expansion models including the polymeric flow [3,4] and the multigrain models [5,6], considering heterogeneous multiple active sites on the catalyst surface and fragmentation phenomenon, have emerged in the literature.

The expansion models consider that polymeric particle, called macroparticle, are made from catalyst fragments, called microparticles. When polymerization is started and polymer produced, polymer chains surround the microparticles and hold microparticles together to form a macroparticle.

In the polymeric flow model, the catalyst microparticles are dispersed in a polymeric continuum and the growing polymer particles are assumed nonporous, subsequently one diffusion coefficient is practical [3,4].

Galvan et al. [7] have presented the modified polymeric

flow model with two different active site types and catalyst deactivation during the heterogeneous Ziegler-Natta polymerization. They found that the increase of polydispersity mainly depends on the presence of two types of active sites. Incorporating a first order deactivation rate into the catalyst kinetic rate equation eliminates the possible diffusion limitations without significantly changing the molar mass and polydispersity of the polymer.

The multigrain model, MGM, is probably the most comprehensive model within all; particularly, it is based on the experimental microscopic observations and applies all the phenomena during the polymerization. The MGM considers three levels of monomer mass and heat transfer: mass and heat transfer at the external boundary layer into the pores of macroparticle, transfer at the macroscale in the interstices between microparticles, and transfer at the microscale within the microparticles.

It can be assumed and also investigated that the heat transfer limitations are negligible for gas and slurry phase in micro and macro levels. However, mass transfer resistances are still important in macroparticle for any polymerization system, specially over all of the highly active and large size catalysts [5,6]. In fact, monomer concentration profile is insignificant for microparticle in slurry phase polymerization.

Sarkar and Gupta [8] proposed a model called polymeric multigrain model (PMGM) that combines features of the multigrain model with some features of the simplified flow model. The authors stated a significant computational time reduction without significant error increase of results in PMGM model. They found that PMGM can predict the polydispersity values higher than that of the multigrain model predictions for single site and Deactivating catalysts. *Sarkar and Gupta* [9] also presented an efficient algorithm to improve CPU time calculation in PMGM computer solver program. However, PMGM is not able to predict polymerization rate as well as MGM model.

Hutchinson et al. [10] have improved MGM for modeling of the particle growth and morphology in copolymerization system. But one of its shortcomings is the complexity of the equations and consequently long time numerical computations for the executive program, which makes it inappropriate for polymerization process application.

Soares and Hamielec [11] have presented the polymeric multilayer model (PMLM) which seems to be less complex than the previous models. In this model, the macroparticle is divided into concentric spherical layers as well as MGM and PMGM; they, also, considered presence of no microparticle for simplification of their model. The model also considers that all layers of the growing particles have the same concentration of the active sites at early step of the polymerization.

Recently, Kanellopoulos *et al.* [12] have developed a mathematical model to study some effective parameters on particle growth and morphology in gas phase olefin polymerization. Authors called their model as the random-pore polymeric flow model. They considered internal and external mass transfer resistances by applying generalized diffusion equation for monomer concentration in polymer phase.

In this study, a new model have been developed to predict particle growth, morphology, the effective parameters on the broadening of the molecular distribution (MWD), average number and molecular weights, isotacticity index and bulk density of polymer. The model is a combination of the polymeric multigrain model (PMGM) [8] and the polymeric multilayer model (PMLM) [11].

First, we have used PMGM and PMLM to drive a more realistic and reduced run time model. In this modeling, we have applied some advantages of PMGM which considers different experimentally observed phenomena in early step and through the polymerization. In addition, we have used PMLM model advantages that are widely used in the kinetic correlations. After that, the results obtained from the new combined model have been compared with those of other important models in the literature.

MODELING

The most acceptable comprehensive model for growing particle can be shown in Fig. 1 schematically. As stated earlier, fragmentation of catalyst particles occurs at early stage of the polymerization. The fragments stay together with surrounding polymer chains and form a macroparticle. To design the model, we consider the macroparticle of N layers in which every layer has been filled out with N_i microparticles, which can be calculated by the following equation:

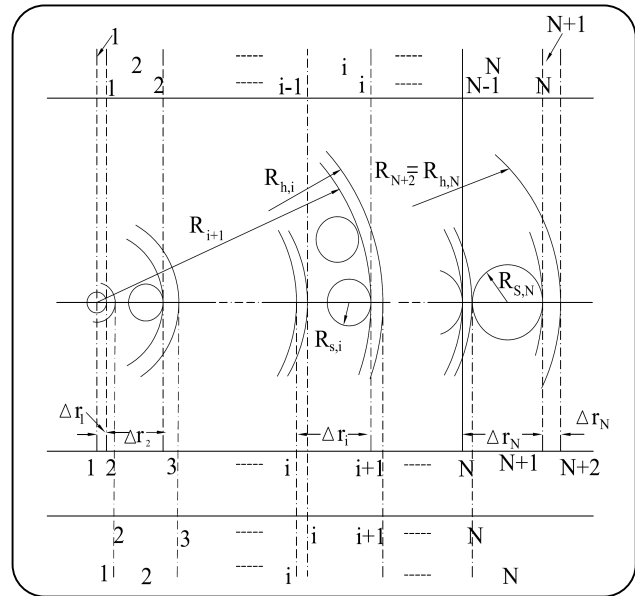


Fig. 1: Schematic of model similar to PMGM.

$$N_i = 6(1 - \varepsilon^*) \frac{\left[R_{s,i} + 2 \sum_{j=2}^{i-1} R_{s,j} + R_{s,i} \right]^2}{R_{s,i}^2} \quad (1)$$

for $i = 2, 3, \dots, N$

Where ε indicates void fraction of the particles; it can be considered as a constant value in all macroparticle layers or can be assumed to be a function of the layer radius. It is evident that only one fragment must be present for the first layer.

$R_{s,i}$ defines the radius of i^{th} fragments which has a typical value in PMGM model, but in the new model it is assumed that the radius of fragments are not the same and can be calculated by a random generator function proposed by Nagel *et al.* [13]:

$$R_{\text{cat.}} = R_{\text{av}} + C(R_{\text{max}} - R_{\text{av}}) \frac{1 - e^{-\left[\frac{(0.5 - \text{Rand})^2}{2} \right]}}{(1 - e^{-0.125})} \quad (2)$$

$$\text{Rand} \leq 0.5; \quad C = -1$$

$$\text{Rand} > 0.5; \quad C = 1$$

$$0 < \text{Rand} < 1.0$$

R_{max} and R_{av} are maximum and average radius of the catalyst fragments, respectively. Typical values for R_{max} and R_{av} are $50 \mu\text{m}$ and $10 \mu\text{m}$, correspondingly.

Fig. 1 shows the imaginary radius of i^{th} layer that we define it by $R_{h,i}$. The catalyst particles can be placed at the mid-points of each imaginary layer.

At time zero, it is assumed there is no monomer diffusion toward catalyst surface to start polymerization, so all the layers have the same size at $t=0$. Whenever polymerization starts, monomer molecules diffuse and reach rapidly to the active sites on the catalyst surface. Indeed, all the microparticles are surrounded by the growing polymer chains. Consequently their size, volume and position are changed. The new positions of all the layers and corresponding macroparticle must be modified according to microparticle volumetric changes. So it is necessary to update all the positions and volumes at any time interval. In addition, any related parameters including the monomer diffusion and the concentration must be renewed at each time interval during the polymerization reaction.

The radial monomer concentration profile can be described by the well-known diffusion-reaction equation in spherical coordinates for macroparticle, given by:

$$\frac{\partial[M_i]_l}{\partial t} = \frac{1}{r_i^2} \frac{\partial}{\partial r_i} (D_i r_i^2 \frac{\partial[M_i]_l}{\partial r_i}) - (R_p)_i \quad (3)$$

$$\text{B.C.1 } r_i = 0; \frac{\partial[M_i]_l}{\partial r_i} = 0$$

$$\text{B.C.2 } r_i = R_i; D_i \frac{\partial[M_i]_l}{\partial r_i} = k_s ([M_i]_b - [M_i]_l)$$

$$\text{I.C. } t = 0 ; [M_i]_l = [M_i]_0 \quad R_i = \phi_0 r_{\text{cat}}$$

M_i denotes the monomer concentration in the polymer or macroparticle; r_i is radial coordinate of the macroparticle; R_i is radius of the macroparticle; r_{cat} indicates radius of the primary catalyst; D_i is effective diffusivity of the monomer in the macroparticle; $[M]_0$ and $[M]_b$ are the initial and the bulk monomer concentrations, respectively; k_s is the external film mass transfer coefficient, and R_p is the volumetric reaction rate in the macroparticle given by:

$$R_p = \frac{3.6 M_w k_p C^* \sum_{i=1}^N (M_{i+1} N_i R_{c,i}^3)}{\rho_c \sum_{i=1}^N (N_i R_{c,i}^3)} \quad (4)$$

where, M_w is molecular weight of the monomer and ρ_c is

Table 1: Kinetic reactions scheme.

Site formation: $N^*(j) + Al \xrightarrow{k_f(j)} N(0, j)$
Initiation: $N(0, j) + M_i \xrightarrow{k_i(j)} N_i(1, j)$
Propagation: $N_i(r, j) + M_k \xrightarrow{k_{pk}(j)} N_k(r+1, j)$
Transfer to Monomer: $N_i(r, j) + M_k \xrightarrow{k_{tmk}(j)} N_k(1, j) + Q(r, j)$
Transfer to cocatalyst: $N_i(r, j) + Al \xrightarrow{k_{tAi}(j)} N_2(1, j) + Q(r, j)$
Transfer to hydrogen: $N_i(r, j) + H_2 \xrightarrow{k_{tHi}(j)} N_H(0, j) + Q(r, j)$ $N_H(0, j) + M_i \xrightarrow{k_{Hi}(j)} N_i(1, j)$ $N_H(0, j) + Al \xrightarrow{k_{HA}(j)} N_2(1, j)$
β -hybride elimination deactivation: $N_i(r, j) \xrightarrow{k_{tsi}(j)} N_H(0, j) + Q(r, j)$ $N_i(r, j) \xrightarrow{k_{ds}(j)} N_d(j) + Q(r, j)$ $N_H(0, j) \xrightarrow{k_{ds}(j)} N_d(j)$ $N(0, j) \xrightarrow{k_{ds}(j)} N_d(j)$
Reaction with impurities: $N_i(r, j) + IM \xrightarrow{k_{dIM}(j)} N_{dIM_H}(0, j) + Q(r, j)$ $N_H(0, j) + IM \xrightarrow{k_{dIM}(j)} N_{dIM_H}(0, j)$ $N(0, j) + IM \xrightarrow{k_{dIM}(j)} N_{dIM}(0, j)$ $N_{dIM_H}(0, j) \xrightarrow{k_a(j)} N_H(0, j) + IM$ $N_{dIM}(0, j) \xrightarrow{k_a(j)} N(0, j) + IM$

the catalyst density, k_p is propagation rate constant and C^* is active site concentration which can be calculated from discretized form of kinetic equations presented in table 1.

The main reaction kinetics includes active site formation, site activation, initiation, propagation, and chain transfer by hydrogen, cocatalyst and monomer. In addition, deactivation of catalyst during time and effects of impurities have been considers. All the kinetic rate constants in the different kinetic models have been applied in our modeling from literatures [10,11,14-16] to compare predicted results.

The Abbreviation symbols shown in table 1 include N^* which is defined as the potential active site of the catalyst; N represents a live polymer chain and Q is a dead polymer chain. $N(0,j)$ is an active site of type j , $N_d(j)$ is a deactivated site of type j , $N_{DIM}(0,j)$ is a site of type j deactivated by impurities, $N_i(r,j)$ is a growing polymer site of type j with length r and the terminal monomer of type i .

In the presented kinetic scheme, $N_T(r,j)$ indicates the total growing polymer sites of type j with length r and $N_H(0,j)$ is defined as a terminated site by hydrogen. Monomer molecules are indicated by M , cocatalyst by Al , hydrogen by H_2 , and impurities by IM . The subscript j is used for an active site of type j , as well as subscripts i and k identify the monomer type.

Similar to equation (3), the microparticle monomer concentration profile and the temperature profile in the micro and macroparticle can be written by the appropriate boundaries. However, we have supposed isothermal conditions in both levels in our modeling.

To apply the partial differential equation (3) (PDE) in the modeling, it should first be discretized. This means converting of PDE into a set of ordinary differential equations (ODEs) used for numerical analysis methods. The converted ODEs equations have been presented in equation (5) and it must be noted that the number of equations in ODEs set equals the number of layers.

This model was implemented as a MATLAB M-function and solved with a differentiation subroutine called ODE15S which is usually used for stiff differential equations.

$$\frac{dM_i}{dt} = \frac{6D_{eff,i}(M_2 - M_i)}{(\Delta r_i)^2} - R_{v,i} \quad (5)$$

$$i = 2, 3, \dots, N_s + 1$$

$$\frac{dM_i}{dt} = \frac{2D_{eff,i}}{\Delta r_i + \Delta r_{i-1}} \begin{bmatrix} M_{i+1} \left(\frac{1}{\Delta r_i} + \frac{1}{R_i} \right) \\ -M_{i+1} \left(\frac{1}{\Delta r_i} + \frac{1}{\Delta r_{i-1}} \right) \\ M_{i+1} \left(\frac{1}{\Delta r_{i-1}} + \frac{1}{R_i} \right) \end{bmatrix} - R_{v,i}$$

It is observed that the diffusional resistance $1/D_{eff}$ in the macroparticle decreases while the polymerization progresses [8]. Therefore, the effective diffusion

coefficient, D_{eff} , is correlated according to any layer radius as follows:

$$R_{v,i} = \frac{k_p C^* M_i N_{i-1} (R_{s,i-1})^3}{(R_{h,i}^3 - R_{h,i-1}^3)} \quad (6)$$

$$D_{eff,i+1} = D_1 \frac{(R_{h,i}^3 - R_{h,i-1}^3)}{N_i R_{s,i}^3} ; i = 2, 3, \dots, N + 1$$

The Average monomer concentration in each layer is necessary for computing the population balance equations of all active species, equations (8) to (19), at any new time interval. The volume of each layer is updated according to the amount of formed polymer in the same time interval. Volume changes affect the radius of every layer, hence the radii of all the layers need to be renewed in each time interval. Also, to calculate particle growth factor during polymerization time, monomer concentration in each layer of polymer particle must be estimated. The simplified approach is noticed in the following derivations.

At a time interval, t to $t + \Delta t$, the volume of polymer produced by catalyst particles can be given by:

$$\Delta V = k_p C^* M_{i+1} (N_i \frac{4\pi}{3} R_{s,i}^3) M_w (\Delta t) / \rho_p \quad (7)$$

that ρ_p is density of the polymer.

The monomer and temperature profiles, for non isothermal case, are recalculated for the new boundary positions and the procedure is repeated for the next time interval. The population balances derived for each layer are the same as would be used in a model without mass and heat transfer resistances. If those resistances are found to be of little importance, the same equations can still be used with the bulk monomer concentrations.

Population balance equations

Population balances for the active species are defined for each concentric layer. The following modeling assumptions are considered

1- Isothermal condition is assumed in radial position as well as all over the polymerization time.

2- In kinetic polymerization, chain transfer to hydrogen is considered the most important transfer reaction of the entire polymerization if hydrogen is present in reactor feed. On the other hand, chain transfer

to cocatalyst is assumed as the main transfer reaction in the absence of hydrogen.

3- Catalyst deactivation has a first order kinetic rate.

4- There are no radial concentration gradients for hydrogen, cocatalyst and external donor components.

5- Quasi steady state approximation (QSSA) is applied for concentration profile of all active species with short living time such as: $N(0,j)$, $N_H(0,j)$ and $N_{DIM}(0,j)$. By using QSSA it is possible to modify the stiffness of several differential equations to the nonstiff equations; therefore execution time for solving numerical analysis subroutine is reduced significantly.

6- Properties of the produced polymer are estimated by applying method of moments; and the output results of the simulation are the average properties of polymers.

In case of copolymerization system Pseudo kinetic rate constants are used in population equations to simplify the mathematical relations [10].

By applying the proposed kinetic scheme shown in Table 1, the population balances for the living polymer of chain length r can be written:

$$\frac{dN_T}{dt}(1,j) = k_i(j)N(0,j)\bar{M}_T + k_H(j)N_H(0,j)\bar{M}_T + \quad (8)$$

$$k_{tm}(j)\bar{M}_T \left\{ \sum_{r=1}^{\infty} N_T(r,j) - N_T(1,j) \right\} + k_{HA}(j)N_H(0,j)A +$$

$$k_{tA}(j)A \left\{ \sum_{r=1}^{\infty} N_T(r,j) - N_T(1,j) \right\} -$$

$$N_T(1,j) \left\{ k_p(j)\bar{M}_T + k_{tH}(j)H_2 \right. \\ \left. + k_{ts}(j) + k_{ds}(j) + k_{dIM}(j)IM \right\}$$

For $r \geq 2$ equation (9) is given as following:

$$\frac{dN_T}{dt}(r,j) = k_p(j)\bar{M}_T \{N_T(r-1,j) - N_T(r,j)\} - \quad (9)$$

$$N_T(r,j) \left\{ k_{tm}(j)\bar{M}_T + k_{tH}(j)H_2 \right. \\ \left. + k_{tA}(j)A + k_{ts}(j) + k_{ds}(j) + k_{dIM}(j)IM \right\}$$

The molar balance for all the chains of living polymer, the zeroth moment, is obtained by summing equation (9) from length 2 to infinity plus equation (8):

$$\frac{dY_0}{dt}(j) = K_I(j) - \{K'_T(j) + K_D(j)\}Y_0(j) \quad (10)$$

$$Y_0(j) = \sum_{r=1}^{\infty} N_T(r,j) \quad (11)$$

$$K_I(j) = \bar{M}_T \{k_i(j)N(0,j) + k_H(j)N_H(0,j)\} + \quad (12)$$

$$k_{tA}(j)N_H(0,j)A$$

$$K'_T(j) = k_{tH}(j)H_2 + k_{ts}(j) \quad (13)$$

$$K_D(j) = k_{ds}(j) + k_{dIM}(j)IM \quad (14)$$

The first and second moments of the living polymer are obtained by multiplying equation (9) by r and r^2 , respectively; and then, summation of these new equations from length 2 to infinity plus equation (8):

$$\frac{dY_1}{dt}(j) = Y_0(j) \left\{ \begin{array}{l} k_p(j)\bar{M}_T \\ + k_{tm}(j)\bar{M}_T \\ + k_{tA}(j)A \end{array} \right\} - \quad (15)$$

$$\{K_T(j) + K_D(j)\}Y_1(j) + K_I(j)$$

$$\frac{dY_2}{dt}(j) = Y_0(j) \left\{ \begin{array}{l} k_p(j)\bar{M}_T \\ + k_{tm}(j)\bar{M}_T \\ + k_{tA}(j)A \end{array} \right\} + 2k_p(j)\bar{M}_T Y_1(j) - \quad (16)$$

$$\left\{ \begin{array}{l} K_T(j) \\ + K_D(j) \end{array} \right\} Y_2(j) + K_I(j)$$

Similar to living polymer chains, the population balance equations for dead polymer chains and expression for zero moment can be obtained as the following equations,

$$\frac{dX_0}{dt}(j) = \{Y_0(j) - N_T(1,j)\} \{K_T(j) + K_D(j)\} \quad (17)$$

$$X_0(j) = \sum_{r=2}^{\infty} Q(r,j) \quad (18)$$

Furthermore, equation (19) for the first and second moments of the dead polymer is obtained as follows:

$$\frac{dX_n}{dt}(j) = \{Y_n(j) - N_T(1,j)\} \{K_T(j) + K_D(j)\} \quad (19)$$

After computing the population balance equations, it is possible to calculate the average properties including molar balances of the active species in the polymerization, total rate of polymerization, number and weight average of the molecular weight, polydispersity index (PDI), isotacticity index and bulk density of polymer.

Molecular weight averages and PDI

Some average values of polymer properties can be estimated by using the method of moments to obtain averages of number (\bar{M}_n) and weigh the molecular weights (\bar{M}_w).

$$\bar{M}_n = \frac{\sum_{j=1}^n \{X_1(j) + Y_1(j)\}}{\sum_{j=1}^n \{X_0(j) + Y_0(j)\}} \quad (20)$$

$$\bar{M}_w = \frac{\sum_{j=1}^n \{X_2(j) + Y_2(j)\}}{\sum_{j=1}^n \{X_1(j) + Y_1(j)\}} \quad (21)$$

Average polydispersity index can also be estimated as follows:

$$\overline{PDI} = \frac{\bar{M}_w}{\bar{M}_n} \quad (22)$$

In the equations mentioned above, $X_i(j)$ is defined as i^{th} moment of the living polymer site of type j and $Y_i(j)$ is defined as i^{th} moment of the dead polymer site of type j .

In table 2 basic flow diagram of computer simulation program has been presented for all the related equations used in modeling.

RESULTS AND DISCUSSION

A reference set of typical values for the modeling parameters reported by some researchers is presented in table 3 [1-11]. Predicted results from the new model have been compared with those of MGM, PMGM, and PMLM. These models are frequently used in the literature to present Ziegler-Natta olefin polymerization particle growth behavior and morphology predictions. However, in each case we have tried to compare the prediction results of the new model with the published ones in the literature.

The radial profiles of monomer concentration are shown in Fig. 2 for all the mentioned models including MGM, PMLM, PMGM and the new one at 0.1 hr of polymerization time. In this case the main parameters for single site catalyst are: $k_p = 500$ lit/mol.s and $c^* = 0.001$ mol/lit.

Table 2: Flow chart for computer simulation program.

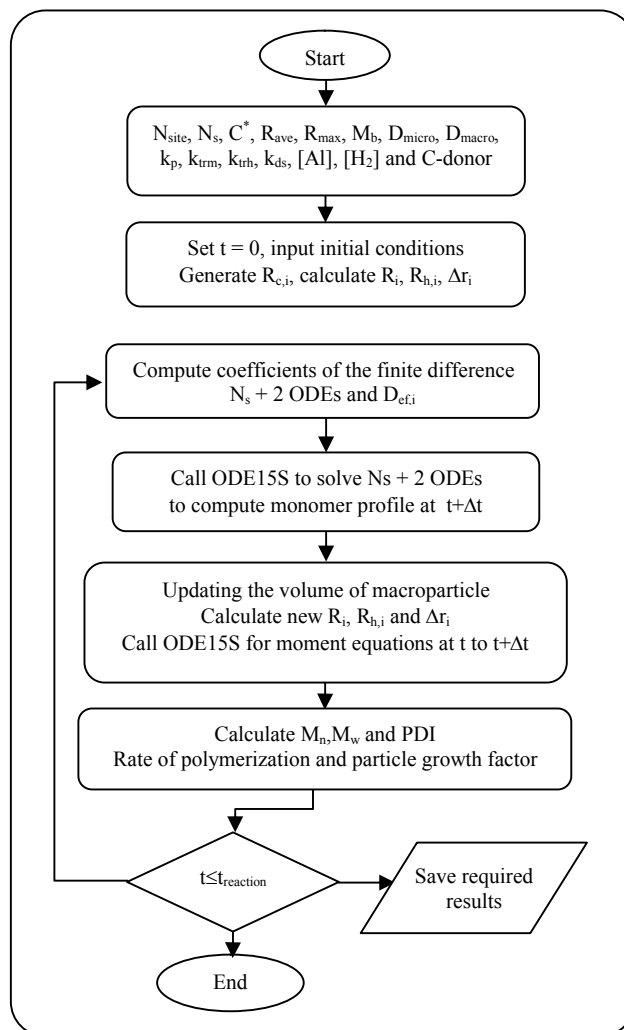


Table 3: Typical values of main modeling parameters [1-11].

Parameter	value	Unit
D_l	10^{-7} - 10^{-5}	cm^2s^{-1}
D_s	10^{-9} - 10^{-7}	cm^2s^{-1}
$[M]_b$	1-4	mol lit^{-1}
$[H_2]$	10^{-6} - 10^{-5}	mol cm^{-3}
C^*	0.1-0.001	mol lit^{-1}
k_p	30-5000	$\text{lit}(\text{mol.s})^{-1}$
k_{trH}	186-1860	$\text{cm}^{3/2}(\text{mol}^{1/2}.\text{s})^{-1}$
R_0	0.01-0.001	cm
N_s	20-50	-
M_w	42/28 Propylene/Ethylene	g/mol
N_{site}	1-3	-
R_{ave}	10-100	μm
Δt	10^{-4} - 10^{-3}	sec

Comparison of the monomer concentration profiles shown in Fig. 2, obtained from different models, displays obviously that the predicted monomer concentration by the new model is less than that of MGM and PMLM model but more than that of the PMGM.

It should be noted that in the same values of main parameters, simulation results of the PMGM radial concentration is far less than other models, so as a result of this shortcoming of PMGM, the published results for PMGM rate of polymerization is not comparable. On the other hand, the simulated results of polymerization rate can be seen in Fig. 3 with corrected PMGM output.

Rate of propylene polymerization by single site non-deactivated catalyst predicted by the new model and the related MGM and PMGM results is shown in Fig. 3. Reference input data for modeling are the same values pointed out in the Fig. 2.

In Fig. 3 it is understandable that all the polymerization rates follow almost the similar trend except that the results of our simulation have shown lower content than that of MGM. The reason of this difference is the lower concentration of monomer in polymeric particle (see Fig. 2).

The higher diffusion coefficient can shift the polymerization rate of the new model close to the rate of MGM model. However, it seems that the value of diffusivity used in MGM model is higher than the values found in experimental works applied in our modeling [17].

Similar results have not been found in the literature for comparison of PMLM results, although, it appears that the rate of polymerization obtained by PMLM can be close to the new simulation results according to the predicted monomer concentration profile shown in Fig. 2.

A comparison of propylene polymerization rate obtained by MGM and the new model has been studied in Fig. 4 for the case of single site first order deactivated catalyst. Simulated results in Fig. 4 approximately states the same predicted polymerization profile by both models but with a little difference especially at the beginning and the end of the polymerization.

Polymer particle growth in olefin polymerization is one of the most important issues in morphological studies of the polymer particle during polymerization. The growing polymer particle profile has been simulated for PMLM and our modeling in Fig. 5. Evaluation of the results in Fig. 5 explains the good agreement for the

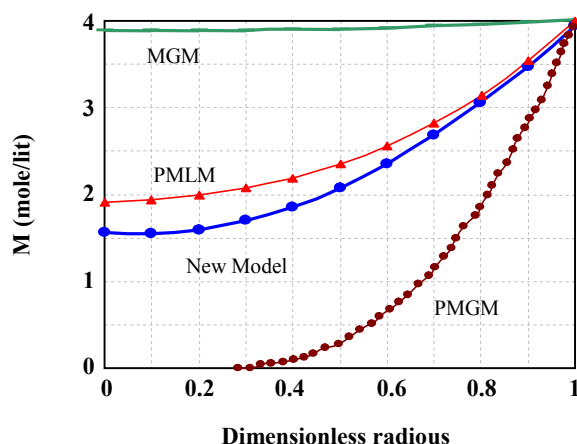


Fig. 2: Radial monomer concentration profile, at 0.1 hr polymerization time for $M_b=4$ mole/lit and $D_l=10^{-6}$ cm^2/s .

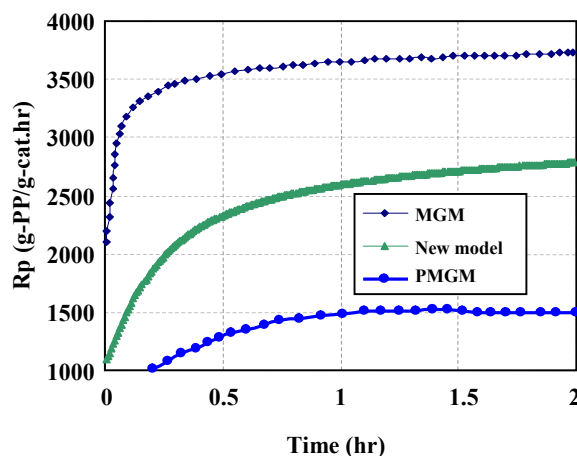


Fig. 3: Polypropylene polymerization rate profile predicted by MGM, PMGM and our simulation for non-deactivated catalyst at $k_p = 660$ lit/moll.s and $C^* = 10^{-5}$ mol/g-cat.

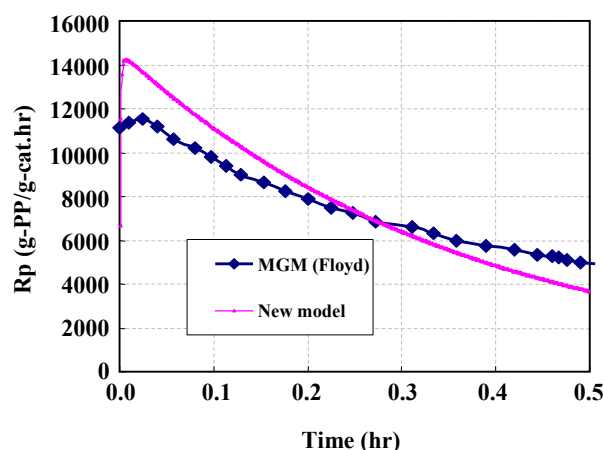


Fig. 4: Profile of polymerization rate of the new model and MGM with reference value in [14].

particle growth factor predicted by the mentioned models. However, because of the lack of exact experimental data, it is not possible to make precise judgment about the correct trend of particle growth profile in among the published results up to now. Hence, in this case we can only make qualitative comparison of the behavior of simulated results to conclude which one is close to real data. Related data for MGM and PMGM were not have found in the literature to compare corresponding results.

The simulated results obtained by the new model and PMLM for number average molecular weight, M_n , are presented in Fig. 6. This fig. shows that predicted results are in good agreements with each other. Furthermore, we found close results with the MGM model which have not been presented here [18].

Predicted polydispersity index, PDI, of the polypropylene polymerized in slurry phase for a three active sites non-deactivated catalyst in absence of hydrogen are shown in Fig. 7. Final average PDI value is predicted by our model to be about 2 for a catalyst with single active site, about 4 for a catalyst with two active sites, and close to 6 for the catalyst with three different active sites, all of which have the same kinetic characteristic. These results are in a good agreement with PDI presented in the literature for the polypropylene produced by heterogeneous Ziegler- Natta catalysts.

Although we have tried to find a set of experimental data in the literature with which to compare model perditions, we were not able to find any exact set of experimental data with necessary values to be used in the models. However, at the present time we are doing some experiments to get the necessary data for model evaluation and immediately after evaluation we would be able to confirm the simulation results, experimentally [18].

CONCLUSIONS

A new model based on PMGM and PMLM, has been presented and used for simulation of slurry polymerization of propylene, which can be also used for ethylene and other olefin monomers. Comparison of the new model predictions with results of other models in the literature, and also, qualitative comparison with observed experimental behavior show that this model is able to predict almost a correct monomer profile, polymerization

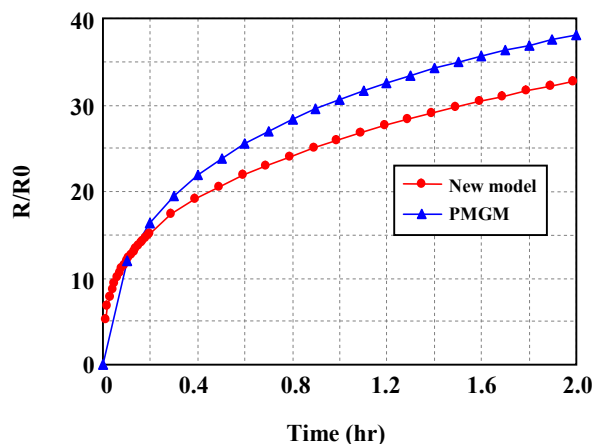


Fig. 5: Simulation results of particle growth profile.

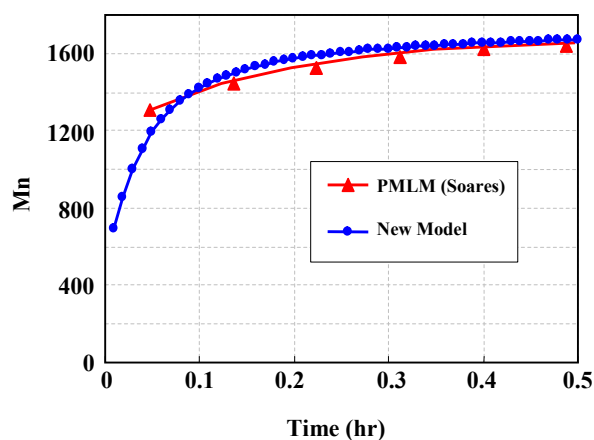


Fig. 6: Number average molecular weight predicted by the same parameters of PMLM Model [11].

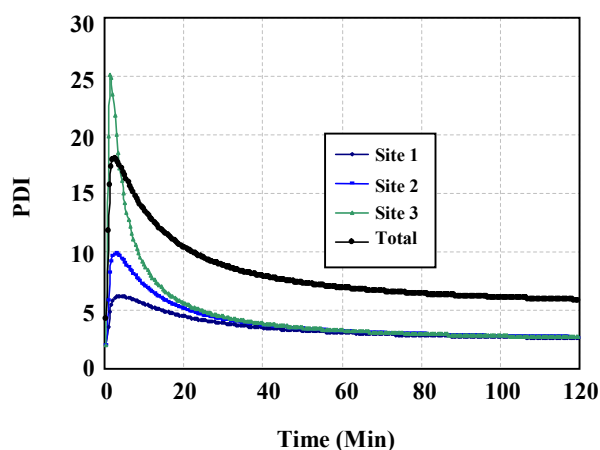


Fig. 7: simulation results for polydispersity index in 3 type-sites catalyst with the same $C^* = 10^{-5}$ mol/g-cat. and $k_p(1) = 500$, $k_p(2)=50$ and $k_p(3) = 5000$ lit/mol.s.

rate, particle growth factor and some important polymer properties which normally cannot be seen together in previously presented models in the literature, except the MGM. However, the latter model needs a tedious numerical solution of complicated equations, and it is not applicable for real situation such as industrial plants. Therefore, it seems that this model can be used as an effective one for simulation of olefin homo and copolymerization in the gas, slurry and bulk phases in different reactors.

Received : 24th July 2006 ; Accepted : 13th January 2008

REFERENCES

- [1] Agarwal, U.S., Modelling Olefin Polymerization on Heterogeneous Catalyst: Polymer Resistance at the Microparticle Level, *Chemical Engineering Science*, **53**, 3941 (1998).
- [2] Boor, J., "Ziegler-Natta Catalysts and Polymerization", Academic Press, New York (1979).
- [3] Singh, D. and Merrill, R. P., Molecular Weight Distribution of Polyethylene Produced by Ziegler-Natta Catalysts, *Macromolecules*, **4**(5), 599 (1971).
- [4] Schmeal, W.R., Street, J.R., Polymerization in Expanding Catalysts, *AIChE J.*, **17** (5), 1189 (1971).
- [5] Floyd, S., Choi, K Y., Taylor, T. W. and Ray, W. H., Polymerization of Olefins through Heterogeneous Catalysis, IV. Modeling of Heat and Mass Transfer Resistance in the Polymer Particle Boundary Layer, *Journal of Applied Polymer Science*, **31**, 2231 (1986a).
- [6] Floyd, S., Choi, K. Y., Taylor, T. W. and Ray, W. H., Polymerization of Olefins through Heterogeneous Catalysis, III. Polymer Particle Modeling with an Analysis of Intraparticle Heat and Mass Transfer Effects, *Journal of Applied Polymer Science*, **32**, 2935 (1986b).
- [7] Galvan, R. and Tirrell, M., Molecular Weight Distribution Predictions for Heterogeneous Ziegler-Natta Polymerization using a Two-Site Model, *Chemical Engineering Science*, **41**, 2385 (1986).
- [8] Sarkar, P., Gupta, S.K., Modelling of Propylene Polymerization in an Isothermal Slurry Reactor, *Polymer*, **32** (15), 2842 (1991).
- [9] Sarkar, P., Gupta, S.K., Simulation of Propylene Polymerization: an Efficient Algorithm, *Polymer*, **33** (7), 1477 (1992).
- [10] Hutchinson, R. A., Chen, C. M. and Ray, W. H., Polymerization of Olefins through Heterogeneous Catalysis, X. Modeling of Particle Growth and Morphology, *Journal of Applied Polymer Science*, **44**, 1389 (1992).
- [11] Soares, J.B.P., Hamielec, A.E., General Dynamic Mathematical Modeling of Heterogeneous Ziegler-Natta and Metallocene Catalyzed Copolymerization with Multiple Site Types and Mass and Heat Transfer Resistances, *Polym. Reac. Eng.*, **3**(3), 261 (1995).
- [12] Kanellopoulos, V., Dompazis, G., Gustafsson, B. and Kiparissides, C., Comprehensive Analysis of Single-Particle Growth in Heterogeneous Olefin Polymerization: The Random-Pore Polymeric Flow Model, *Ind. Eng. Chem. Res.*, **43** (17), 5166 (2004).
- [13] Nagel, E. J., Kirillov, V. A. and Ray, W. H., Prediction of Molecular Weight Distributions for High-Density Polyolefins, *Industrial & Engineering Chemistry Product Research and Development*, **19**, 372 (1980).
- [14] Floyd, S., Heiskanen, T., Taylor, T. W., Mann, G. E. and Ray, W. H., Polymerization of Olefins through Heterogeneous Catalysis, VI. Effect of Particle Heat and Mass Transfer on Polymerization Behavior and Polymer Properties, *Journal of Applied Polymer Science*, **33**, 1021 (1987).
- [15] De Carvalho, A.B., Gloor, P.E., Hamielec, A.E., A Kinetic Mathematical Model for Heterogeneous Ziegler-Natta Copolymerization, *Polymer*, **30**, 280 (1989).
- [16] McAuley, K.B., MacGregor, J.F., Hamielec, A.E., A Kinetic Model for Industrial Gas-Phase Ethylene Polymerization, *AIChE J.*, **36** (6), 837 (1990).
- [17] Li, J., Tekie, Z., Mizan, T. I. and Morsi, B. I., Gas-Liquid Mass Transfer in a Slurry Reactor Operating Under Olefinic Polymerization Process Conditions, *Chemical Engineering Science*, **51**(4), p. 549 (1996).
- [18] Dashti, A., Modeling of Particle Growth and Morphology of Slurry Phase Polypropylene Polymerization Using Heterogeneous Ziegler Natta Catalysts, M.Sc. Thesis, Sharif University of Technology, Tehran, (2003).